

# DIFFERENTIATION OF EPICUTICULAR WAX COMPONENTS ON THE SURFACE OF ARABIDOPSIS ORGANS

by TOF-SIMS Imaging

## OVERVIEW

The ability to elucidate the origin and composition of a distinguishing mass spectral feature is an essential function of time-of-flight secondary ion mass spectrometry (TOF-SIMS) in addition to the unique capability to visualize chemical information in a spatially resolved manner. In most instances, the samples or specimens being interrogated have some curvature or are otherwise topographically rough. Rough and curved surfaces present a challenge in TOF-SIMS imaging due to the effects of topography on the kinetic energies and

trajectories of secondary ions. These effects are commonly referred to as topographic contrast. The ion optics of the PHI *nanoTOF*'s TRIFT analyzer are optimized for chemical imaging and mass spectrometry of topographically rough specimens in that both a wide angular acceptance and a large depth-of-field are inherent in the design [1-3].

In this Note, we demonstrate the use of the PHI TRIFT V *nanoTOF* to extract chemical information associated with a series of non-woody botanical specimens. The sample set consists of *Arabidopsis thaliana* organs

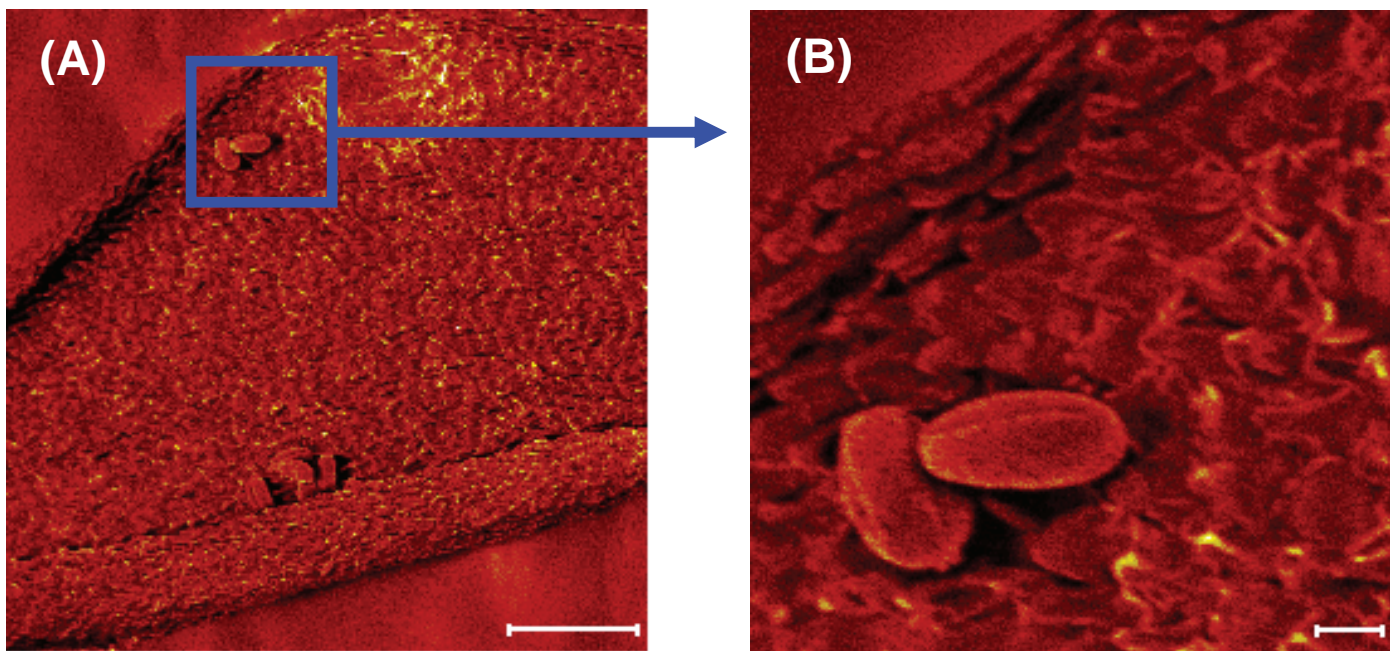


Figure 1: (A) Total ion (+SIMS) image of a petal of an *Arabidopsis* flower. The field-of-view (FOV) is 500  $\mu\text{m} \times 500 \mu\text{m}$  (scale bar is 100  $\mu\text{m}$ ). Two areas are present containing spores. (B) Total ion (+SIMS) image of spores on the *Arabidopsis* petal at higher magnification. The FOV is 100  $\mu\text{m} \times 100 \mu\text{m}$  (scale bar is 10  $\mu\text{m}$ ). The spores are readily observed in the lower-left portion of the image, and other cells of the petal are also clearly visible. In each image, the mounting adhesive is also observed off the edge of the petal.

including flower, stem, leaf-top and leaf-bottom specimens. The morphological roughness ranges from 20 - 50  $\mu\text{m}$  on the nominally flat flower petals, to more than 30  $\mu\text{m}$  on the curved surface of the approximately 150  $\mu\text{m}$  diameter stem, to greater than 200  $\mu\text{m}$  on the leaf specimens. A primary focus of this study is the differentiation of epicuticular waxes present at the surface of each *Arabidopsis* organ [4,5]. The salient features of the TRIFT mass spectrometer are utilized to distinguish the chemistries associated with the different *Arabidopsis* organs, and to confirm via chemical imaging the identification of a mass spectral feature as a molecular ion or molecular fragment ion of an epicuticular wax component.

## EXPERIMENTAL

Four specimens of *Arabidopsis*, including a pressed flower, a stem section, a whole leaf mounted with the adaxial (top) surface exposed, and a whole leaf mounted with the abaxial (bottom) surface exposed, were analyzed by TOF-SIMS. Each specimen had been previously dehydrated and mounted using double-sided adhesive; each specimen was introduced to vacuum and analyzed by TOF-SIMS in the as-received state.

An unbunched 30 keV  $\text{Au}^+$  primary ion beam was used to acquire chemical images of the *Arabidopsis* specimens in both secondary ion polarities. A raw data stream file was collected in each secondary ion polarity to allow further post-acquisition evaluation (i.e. retrospective analysis)

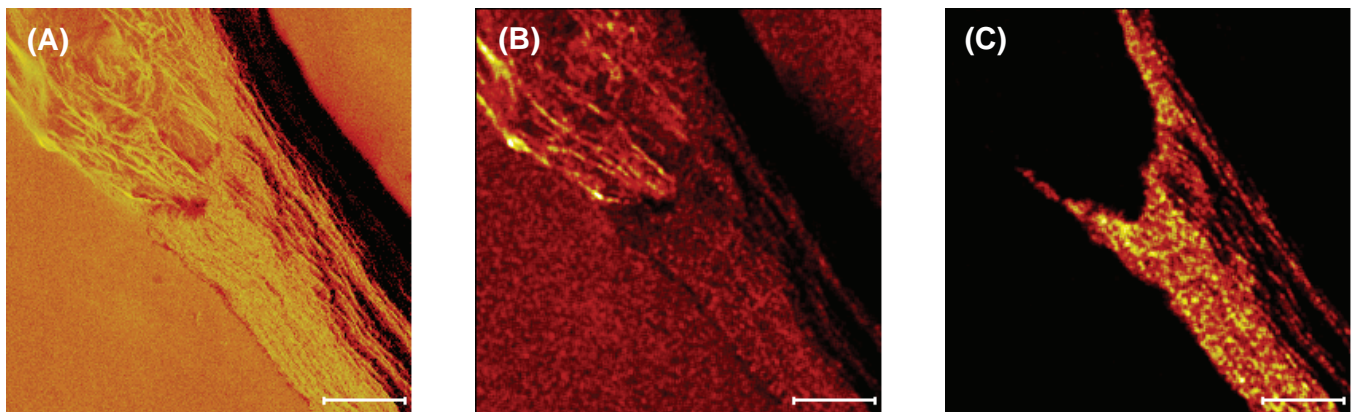


**Figure 2:** (A) Total ion (+SIMS) image of an *Arabidopsis* stem. The stem is approximately 150  $\mu\text{m}$  in diameter. Secondary ion signal is collected from the entire surface of the stem that is probed by the primary ion beam, and the mounting adhesive surrounding the specimen is also observed. (B) Chemical image of PDMS ( $\text{C}_5\text{H}_{15}\text{Si}_2\text{O}^+$ , 147  $\text{m/z}$ ) showing that PDMS from the surrounding adhesive has contaminated the stem surface. (C) Chemical image of an epicuticular wax component (423  $\text{m/z}$ ) localized to the outer surface of the stem. The FOV in each image is 500  $\mu\text{m}$  x 500  $\mu\text{m}$  (scale bar is 100  $\mu\text{m}$ ).

of the data. All chemical images and mass spectral data were collected operating the  $\text{Au}^+$  primary ion beam at DC currents of either 0.5 nA or 1.5 nA. A post-acceleration of 20 kV on the secondary ion detector was used for higher molecular ion sensitivity in each secondary ion polarity. The raw data stream files were collected for 15 minutes each, and a digital raster of 256 pixels x 256 pixels was used for each acquisition. The primary ion dose density (PIDD) is necessarily variable and is dependent on the raster size (i.e. field-of-view) of each image, but in any case does not exceed  $2.9 \times 10^{12} \text{ Au}^+/\text{cm}^2$  which is well within the static limit for TOF-SIMS analysis. Charge compensation during analysis was accomplished using PHI's patented dual-beam charge neutralization technology.

## RESULTS

Total ion images of the *Arabidopsis* flower petal are presented in Figure 1. The corresponding mass spectra of the flower petal are given in Figures 4 and 5. Notice in Figure 1A that numerous structural features of the petal are clearly visible and include several spores on the surface. A magnified image of the area indicated in Figure 1A is given in Figure 1B where the details of the spores and the epidermal cells at the edge of the petal are clearly recognized. In these images it may also be observed that the secondary ion signal is relatively uniform across the surface of the petal and the spores, and signal is also collected from the adhesive tape surrounding the flower petal. That is to say, the effects of signal

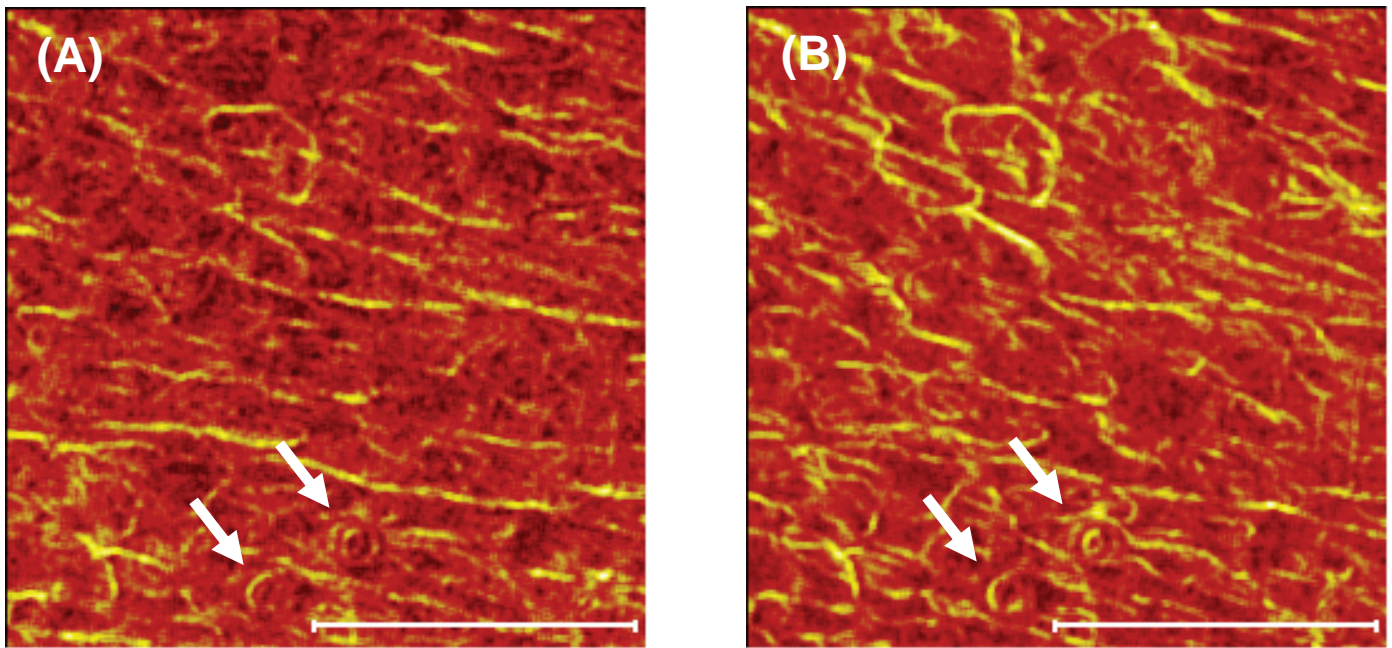


**Figure 3:** (A) Total ion (-SIMS) image of an abaxial (bottom) *Arabidopsis* leaf surface. The FOV is 200  $\mu\text{m} \times 200 \mu\text{m}$  (scale bar is 100  $\mu\text{m}$ ). (B) Pulsed primary ion-induced secondary electron (SE) image of an abaxial (bottom) *Arabidopsis* leaf surface acquired simultaneously with the -SIMS data. The FOV is 200  $\mu\text{m} \times 200 \mu\text{m}$  (scale bar is 100  $\mu\text{m}$ ). There are several respiratory pores present, two of which have been marked with arrows are particularly discernible near the left edge of the scale marker(s).

variation as a function of surface geometry (topographic contrast) are minimized such that secondary ion signal is collected from the entire field-of-view. This is an important analytical advantage of the TRIFT spectrometer, the result of a large depth-of-field, that allows efficient secondary ion collection from morphologically rough surfaces for the purposes of imaging mass spectrometry.

The difficulty associated with achieving uniform secondary ion detection across the curved, or morphologically rough, surface of an insulating specimen has been discussed previously in detail [1-3]. In brief, secondary ions that depart different points of the probed specimen experience different accelerating potentials before entering the mass spectrometer and, therefore, have different kinetic energies. In order to compensate for these topographic effects, an efficient imaging mass spectrometer must have the ability to collect ions having a large dispersion in kinetic energy and to compensate for the effect of kinetic energy on the flight times of ions at each mass-to-charge ( $m/z$ ) ratio. The TRIFT spectrometer, operating in the standard mode, is able to collect secondary ions with a kinetic energy spread of 240 eV and the embedded triple-ESA focuses the secondary ions in time to compensate for differences in kinetic energy.

The necessity of a large depth-of-field for the chemical imaging of a morphologically rough surface is exemplified in Figure 2 where images of the *Arabidopsis* stem are presented. The corresponding mass spectra of the stem are given in Figures 4 and 5. The total ion image in Figure 2A reveals both the surface (i.e. cuticle) and the internal cross-section of the stem; the secondary ion signal arising from the adhesive tape surrounding the stem is also observed. Chemical images may be utilized to determine which mass spectral features arise from the epicuticular region of the stem. A mass peak at 147  $m/z$ , most likely a molecular fragment of PDMS ( $\text{C}_5\text{H}_{15}\text{Si}_2\text{O}^+$ ) based on the measured mass-to-charge ratio, is imaged in Figure 2B. Since this mass spectral feature is present across the entire surface of the stem, and more notably over the surface of the surrounding adhesive, its assignment as a molecular fragment of PDMS is reasonable. Conversely, as observed in Figure 2C, the mass peak at 423  $m/z$  is localized to the cuticular region of the stem and is likely a component of epicuticular wax.

A total ion image of the abaxial (bottom) surface of an *Arabidopsis* leaf is rendered in Figure 3A. A corresponding pulsed secondary electron image, acquired simultaneously with the secondary ion image data, is shown in Figure 3B. Secondary

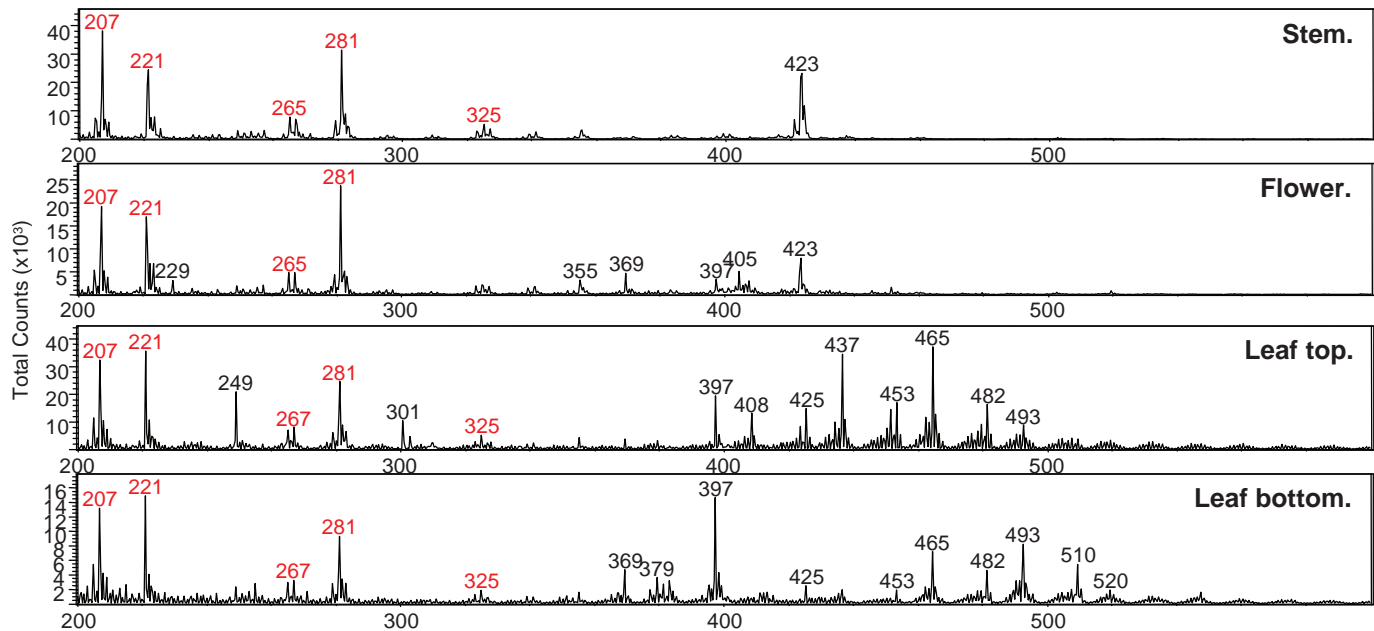


**Figure 4:** Positive secondary ion polarity (+SIMS) mass spectra of the *Arabidopsis* organs in the mass range of 200 – 600  $m/z$ . The molecular and molecular fragment ions of the epicuticular wax components are most prominent in the mass spectra at  $m/z$  > 350. Peaks arising from the adhesive, i.e. PDMS, are indicated in red.

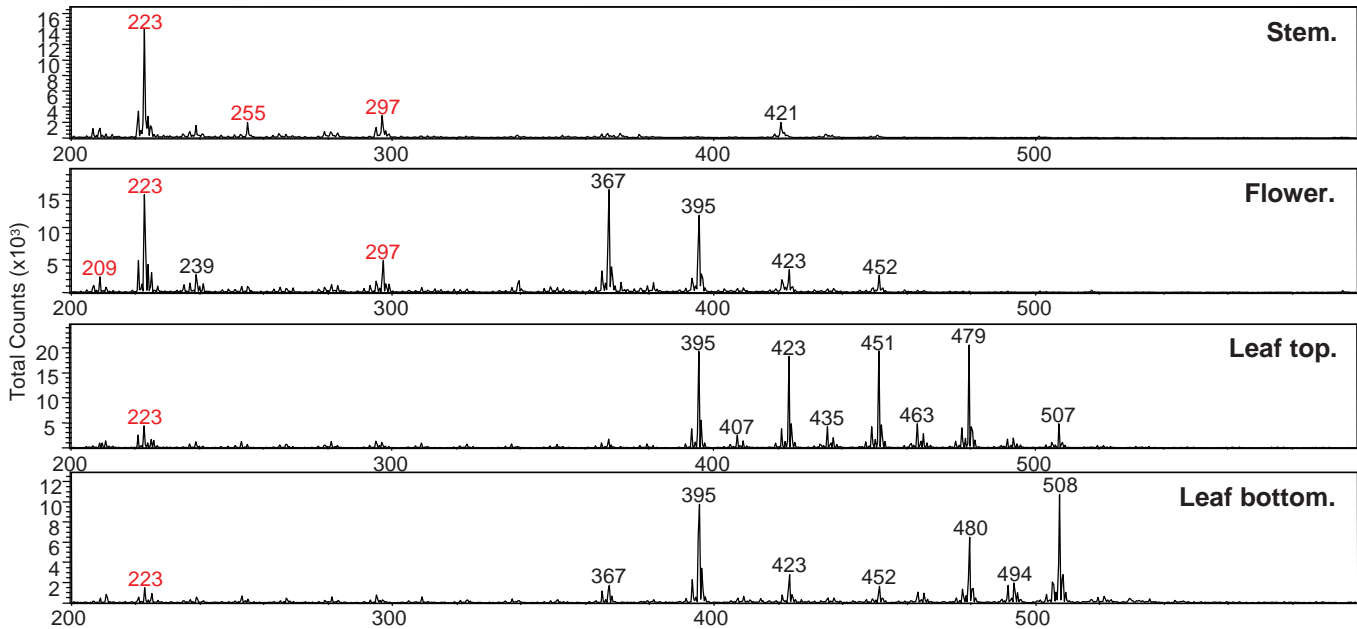


**Figure 5:** Negative secondary ion polarity (-SIMS) mass spectra of the *Arabidopsis* organs in the mass range of 200 – 600  $m/z$ . The molecular and molecular fragment ions of the epicuticular wax components are most prominent in the mass spectra at  $m/z$  > 350. Peaks arising from the adhesive, i.e. PDMS, are indicated in red.

electron imaging is useful because it provides a high contrast method for imaging topographic features and morphological roughness. It is not generally possible to obtain DC beam-generated secondary electron images from insulating specimens because the resulting space-charge produces severe distortion of the image, or no image at all. The TRIFT spectrometer is uniquely capable of collecting secondary electron images from insulating and conducting specimens alike during the pulsed acquisition mode, i.e. during mass spectrometric operation. This pulsed mode collection of secondary

electron images occurs by deflecting the primary ion-generated secondary electrons, which have a much higher velocity than the more massive secondary ions, into a secondary electron detector (SED) located in the flight path of the TRIFT spectrometer while passing the secondary ions to the dual multichannel plate (DMCP) detector. The most notable features present in the secondary ion and secondary electron images of the abaxial leaf surface in Figure 3, besides the obvious morphological roughness, are the respiratory pores. Two such pores are identified with arrows in Figure 3. The mass spectra of the abaxial leaf surface are given in Figures 4 and 5.

TOF-SIMS images of the adaxial (top) surface of an *Arabidopsis* leaf are not presented in this Note; nevertheless, the mass spectra are included in Figures 4 and 5 along with the spectra of the abaxial leaf surface, the stem, and the flower petal. For each organ of *Arabidopsis* examined by TOF-SIMS there is a persistent background of relatively short-chain silicones from the adhesive tape used to mount each specimen. What is particularly notable among the mass spectra from the various *Arabidopsis* organs is that the composition of the epicuticular waxes, while similar, is quite distinct. This observation corresponds well with prior work [4,5]. A magnified image of the area about the respiratory pores indicated in Figure 3 (data not presented here) reveals the respiratory pores to be clearly resolved from the adjacent topography. The pores have dimensions of approximately 7  $\mu\text{m}$  in length and approximately 1  $\mu\text{m}$  in width [6]. Region-of-interest (ROI) mass spectra generated from within and outside the respiratory pores (data not presented here) indicate that the epicuticular wax components within the pores is compositionally distinct from that surrounding the pores. Though the signals from such a small number of image pixels is low, the comparative measurement is made with confidence owing to the low noise and low spectroscopic background characteristics of the TRIFT spectrometer.

## CONCLUSION

Three unique and analytically powerful characteristics of the *nanoTOF* and its TRIFT spectrometer were demonstrated in the context of imaging topographically rough and

morphologically diverse organs of *Arabidopsis* and observing the distinct differences in the composition of the epicuticular waxes via the resulting mass spectra. (1) The superior angular acceptance and depth-of-field of the TRIFT spectrometer enables the efficient collection of secondary ions from all parts of topographically rough samples that are interrogated by the primary ion beam. (2) The collinear arrangement of the secondary electron and the secondary ion detectors in the TRIFT spectrometer allows the collection of secondary electron images from insulating samples during pulsed TOF-SIMS data acquisition. Thus, the secondary electron and the TOF-SIMS chemical images are in perfect registry. (3) The realization of high quality mass spectra collected from specimens having large differences in topography and morphology is possible because of the exceptionally low noise and low spectroscopic background of the TRIFT spectrometer, even at a high (i.e. 20 kV) post-acceleration voltage.

## ACKNOWLEDGEMENTS AND REFERENCES

We would like to thank Dr. Reinhard Jetter of the Departments of Chemistry and Botany at the University of British Columbia for providing the *Arabidopsis* specimens.

- [1] *Imaging Additives on Human Hair with the PHI nanoTOF*, Application Note, (2009) Physical Electronics.
- [2] *Chemical Imaging on Particles with the PHI nanoTOF*, Application Note, (2009) Physical Electronics.
- [3] *Quantitative Analysis of Topographic Effects on Conductive Surfaces*, Technical Bulletin (2009) Physical Electronics.
- [4] M.C. Suh, A.L. Samuels, R. Jetter, L. Kunst, M. Pollard, J. Ohlrogge and F. Beisson, *Plant Physio.* **139** (2005) 1649.
- [5] M. Wen and R. Jetter, *J. Exp. Botany* **60** (2009) 1811.
- [6] C. VanMaarseveen and R. Jetter, *Phytochem.* **70** (2009) 899.